

Citation

Bonesso, J.L. and Browne, N.K. and Murley, M. and Dee, S. and Cuttler, M.V.W. and Paumard, V. and Benson, D. et al. 2022. Reef to island sediment connections within an inshore turbid reef island system of the eastern Indian Ocean. *Sedimentary Geology*. 436. <http://doi.org/10.1016/j.sedgeo.2022.106177>

1 **Reef to island sediment connections within an inshore turbid reef island system of the eastern**
 2 **Indian Ocean**

3 **Joshua L. Bonesso**^{1,2,3,4*}, Nicola K. Browne⁵, Matilda Murley^{3,6}, Shannon Dee⁵, Michael V.W. Cuttler^{3,7},
 4 Victorien Paumard^{1,3,8}, Dylan Benson⁵ & Michael O’Leary^{1,3}

5 ¹ School of Earth Sciences, University of Western Australia, Perth, 6009, Australia

6 ² ARC Centre of Excellence for Coral Reef Studies, University of Western Australia, Perth, 6009, Australia

7 ³ UWA Oceans Institute, University of Western Australia, Perth, 6009, Australia

8 ⁴Western Australian Marine Science Institution, Perth, 6009, Australia

9 ⁵ School of Molecular and Life Sciences, Curtin University, Perth, 6102, Australia

10 ⁶ School of Biological Sciences, University of Western Australia, Perth, 6009, Australia

11 ⁷ Oceans Graduate School, University of Western Australia, Perth, 6009, Australia

12 ⁸ Centre for Energy Geoscience, University of Western Australia, Perth, 6009, Australia

13

14 **Keywords:** reef islands; sediment connectivity; carbonates; Indian Ocean; climate change; coral reef

15

16 Corresponding author: joshua.bonesso@research.uwa.edu.au

17

18 **Abstract**

19

20 Reef islands are low-lying sedimentary landforms formed from the accumulation of unconsolidated skeletal
 21 material generated by carbonate-producing reef organisms. The coupling between ecological (extant community
 22 assemblage) and sedimentary processes (sediment composition and supply) that maintain these reef-fronted
 23 landforms make them increasingly sensitive to the impacts of future environmental change. To understand this
 24 interconnection we examine the benthic reef community assemblage and sediment characteristics (composition
 25 and texture) at Eva Island, an inshore turbid reef island system located in the Pilbara region of Western Australia.
 26 Benthic surveys and sediment composition identified molluscs as a unique primary sand-sized sediment
 27 constituent (34% of reef and sediments, respectively), alongside coral, despite low mollusc abundance in the reef
 28 ecology ($n = 94$ extant individuals). This result, alongside homogeneity within reef and island biosedimentary
 29 facies, suggest a coupling between source (reef) and sink (island) environments may exist, with the sediment
 30 reservoir providing suitable sand-grade material for island nourishment. In light of these findings, assuming island

31 building can keep up with rising sea levels, Eva may be resilient to the immediate impacts of climate change.
32 However, dependency on a few primary sediment constituents (molluscs and coral that are sensitive to
33 environmental perturbations) may compromise long-term resilience (over decades), particularly the direct effect
34 on sediment producing habitats and sensitive calcifying organisms under future changing climatic conditions.

35

36 **1. Introduction**

37

38 Coral reef islands are critically important geomorphological features, providing habitable land for human
39 populations and coastal infrastructures (e.g. atoll nations), and a vital habitat for endemic and/or threatened species
40 of flora and fauna (Fuentes et al., 2011; Fossette et al., 2021). Formed largely of unconsolidated accumulations of
41 biogenic sediments (Yamano et al., 2005; Perry et al., 2011; Ford & Kench, 2015; Morgan & Kench, 2016a and
42 b), their low lying elevations (< 5 meters above mean sea level, amsl) and small geographic area (generally < 100
43 ha) make them increasingly susceptible to variations in metocean boundary conditions (Perry et al., 2011; McLean
44 & Kench, 2015). Near-future scenarios of environmental change, which include rising sea levels and changing
45 wave climate, could erode reef-fringed shorelines and inundate islands. Moreover, rapidly increasing sea surface
46 temperatures (SSTs) and ocean acidification may impede reef productivity, growth, and consequentially reef-
47 derived carbonate sediment production, supply and availability, which is critical for island stability (Perry et al.,
48 2011; East et al., 2018; Cuttler et al., 2019).

49

50 Sediment production and supply to reef islands is inherently dependent on the function and productivity of their
51 associated coral reef ecosystems. Not only does the reef provide a structural foundation for island construction, it
52 is also responsible for the production of carbonate sediments, otherwise known as the ‘reef carbonate factory’
53 (Webb and Kench, 2010; Perry et al., 2015; see review by Browne et al., 2021). Shifts in ecological processes
54 (e.g. rate of carbonate production) directly mediate changes in sediment dynamics and have proven to be a critical
55 control on the construction and maintenance of reef-associated sedimentary landforms (Yamano et al., 2000).
56 These sediments primarily originate from: (1) skeletal remains of calcium carbonate-producing reef biota
57 including primary coral framework, secondary calcareous encrusting organisms (CCA, foraminifera, bryozoans)
58 and direct sediment producers (molluscs, echinoids and *Halimeda*); or (2) a by-product of physical and/or
59 biological erosion of the reef framework (Perry et al., 2011; Morgan & Kench, 2016b). Sediments undergo post-
60 mortem breakdown, altering the grains physical (size, shape and density) and hydraulic (durability, shape, density)

61 properties (i.e., the ‘Sorby principle’; Sorby, 1880). Furthermore, the suitability of the material to be selectively
62 transported and deposited on island shorelines is also a function of the local site hydrodynamic processes (Dawson
63 et al., 2012; Cuttler et al., 2017).

64

65 The link between reef ecology and geomorphic development is critical in determining accretionary evolution and
66 long-term morphological response of reef-fringed landforms and coastlines (Dawson & Smithers, 2014; Perry et
67 al., 2015; Morgan and Kench 2016a, 2016b; Cuttler et al., 2019; Browne et al., 2021). Previous research
68 investigating ecological-sedimentary links within reef-island systems has shown that the spatial distribution of
69 island and reefal sediment constituents may closely reflect living reef community assemblages (e.g. Indian Ocean
70 case studies: Smithers, 1994; Morgan and Kench, 2014; Morgan and Kench, 2016). This link is quantified via
71 ‘carbonate sediment budget’ analyses, which is a balance between the biological (e.g. calcium carbonate (CaCO_3)
72 generated by the reef system, bioerosion), physical (e.g. wave stress, cyclone activity) and chemical (e.g.
73 dissolution) processes that influence the production and availability of carbonate sources and their conversion into
74 detrital sediments (see review by Browne et al., 2021). The budget also accounts for transport pathways between
75 sediment source and sink environments (Morgan and Kench, 2014; Cuttler et al., 2019, Browne et al., 2021). It
76 has been well established that reef islands and other reef-fronted coastlines act as a temporary sink and reservoir
77 of sediment (Kench and McLean 2004; Perry et al., 2011). Furthermore, recent studies have highlighted that
78 sediment within these sinks may not solely originate from recent sediment production, but rather, may be a product
79 of old or ‘relict’ material (in the order of 1000’s of years), in which bioeroders (e.g. parrotfish/urchins) break
80 down the reef framework contributing to contemporary sediment generation (Cuttler et al., 2019).

81

82 The Pilbara region contains Australia’s largest sand-island archipelago, including more than 97 islands that are of
83 high ecological (sea bird and marine turtle rookeries), recreational, and commercial value (oil and gas
84 infrastructures). Unlike comparable reef island systems globally (e.g. Maldives archipelago), the Pilbara inshore
85 reef islands are unique because they are fringed by shallow naturally turbid coral reef habitats (Dee et al., 2020)
86 with island landmasses that reach elevations of 18 m or more and volumes of up to 4.7 million m^3 (e.g. Long
87 Island), which is significant, particularly in decreasing the risk from the extrinsic threat from future sea level
88 trajectories (Bonesso et al., 2020). Previous research has focused on identifying and tracking key island sediment
89 constituents within clear water (and pristine) reef island ecosystems. Yet, limited studies have focused on
90 identifying sediment dynamics within naturally turbid reef island systems, highlighting the Pilbara reef island

91 system as an essential case study in resolving this knowledge gap. Further, given turbid coral reefs have been
92 shown to exhibit heightened resilience in the face of extrinsic environmental change, particularly in response to
93 elevated Sea Surface Temperatures (SSTs), understanding their contemporary sediment dynamics is important in
94 the context of reef islands globally and island resilience in the face of future environmental change (Morgan et
95 al., 2017; Browne et al., 2019; Sully, 2020; Cartwright et al., 2021; Zweifler et al., 2021). This may be significant,
96 given that tropical reef systems may tend towards more turbid systems with the impacts from climate change (see
97 review by Zweifler et al., 2021).

98

99 Here, we combine sedimentological (sediment constituent and grain size characteristic analyses), and ecological
100 datasets to determine the (1) primary bioclastic grains responsible for island building in a turbid water reef-island
101 setting; (2) key marine habitats responsible for generating island building sediments and; (3) potential sensitivity
102 of these habitats to environmental change and subsequent impact on sediment generation. It is expected that by
103 resolving the relationship between the ecology (living community assemblages), sediment production rates, and
104 sediment transport processes, that improved and robust predictions on the vulnerability and resilience of islands
105 to future environmental change can be determined.

106

107 **2. Field setting, regional climate and oceanography**

108

109 The location of this study is Eva Island (21°55'19"S, 114°25'55"E), a vegetated sand cay situated off the eastern
110 coast of Exmouth Gulf, which is located at the southern extent of the Pilbara region (Figures 1a & 1b). Eva is
111 small in planform area (14.7 ha, 0.147 km²), with a maximum elevation of 8.6 m above mean sea level (amsl) and
112 a volume of 559,427 m³ (2018 LiDAR survey; Bonesso et al., 2020). The island landmass is situated on top of a
113 limestone platform that is fringed by shallow macroalgal-dominated coral communities along its northern and
114 western margins, beachrock extending off the southern edge and across the north periphery of the landmass, and
115 turbid coral patch reef habitats surrounding the northern and eastern periphery of the limestone platform (Bonesso
116 et al., 2020; Dee et al., 2020). Island planform morphology is roughly circular and characterised by a mobile sand
117 spit located at the southern through eastern island margins, vegetated foredunes and swales, and a central island
118 basin (Figures 2a – e; Bonesso et al., 2020; Cuttler et al., 2020). Recent LiDAR surveys of Eva Island from 2016
119 and 2018, showed the landmass to be geomorphically stable (over a 2-year timeframe), with little to no change in
120 island volume, elevation and planform area (Bonesso et al., 2020).

121

122 The Pilbara region of Western Australia is characterised by a dry sub-tropical climate with humid hot
123 summers (36 - 37°C average maximums from November to April) and mild winters (28 - 29°C average maximums
124 from May to October; Leighton, 2004). The Exmouth Gulf region experiences seasonal and inter-annual
125 variability in wind and wave climate characterised by: (1) long period (peak wave period ~7 – 10 s) ocean swell
126 waves that refracts around the NW cape to enter the Exmouth Gulf from a NNW direction during the austral
127 winter; and (2) short period, local wind-generated waves (peak wave period ~ 5 s) produced by prevailing
128 southerlies (i.e., SSW) during the austral summer (Cuttler et al., 2020; Dufois et al., 2017; Cartwright et al., 2021).
129 The Pilbara is also one of the most cyclone prone regions globally (with approximately 3 tropical cyclones making
130 landfall per year), producing large swell (>5 meter wave height) and storm surge (up to several meters in height),
131 which can cause widespread coastal erosion, increased water turbidity levels and coastal landform destabilisation
132 (Nott and Hubbert, 2005).

133

134 **3. Materials and methods**

135

136 Field data collection was undertaken between the 18th and 24th of October 2020, and aimed at
137 understanding the mechanisms of sediment generation from surrounding sub-reef systems and, therefore, their
138 role in reef island landform accretion and development. This included the collection of surficial sediment samples
139 from the: (1) sub-aerial island landform (i.e., beach, foredune and central island basin); and (2) sub-reef habitats
140 (including limestone platform, patch reef habitats and deeper offshore bare bed sites) to a maximum depth of 12
141 m (i.e., offshore sites). Benthic habitat surveys were conducted for the limestone platform (stratified surveys of
142 outer, middle and inner zones) and sub-reef habitats (max depth of ~ 4 m) to determine abundance and spatial
143 coverage of calcifying reef biota (e.g. corals, molluscs, CCA, *Halimeda* and echinoids). Aerial drone photography
144 of the reef and island was conducted in October 2021 using a DJI Phantom 4 RTK, flying at a maximum altitude
145 of ~120 m (Figure 2).

146

147 *3.1 Surficial sediment collection*

148 Sediments were collected along eight radial transects (E1 – E8; Figure 1c) across Eva island and reef, covering
149 the vegetated island landmass and sub-reef environments (limestone reef platform, patch reef and offshore/bare
150 bed). Surficial sediments samples of ~ 150 g were collected at approximately 50 m intervals along each transect,
151 excavated from the top 10 cm of the island surface and benthos using a small 150 cm³ plastic vial. At reef sites,

152 vials were pressed into the benthos and capped at depth. Island sediment samples were collected from the basin,
153 foredunes, and beach (Figure 1c & 2a). A Van Veen grab sampler was used to recover sediment from the offshore
154 environments to a maximum depth ranging between 7 and 12 m (depending on transect) (Figure 1c). All samples
155 were treated in a dilute solution (10%) of sodium hypochlorite (NaOCl; commercial grade bleach) for 24 to 48
156 hours to remove any residual organics (without altering the integrity and morphology of individual sediment
157 grains). Sediments were then rinsed in freshwater and dried at 60°C for 48 hours prior to processing and laboratory
158 analyses. These samples were used to determine sediment composition and grain size.

159

160 *3.2 Components analysis and grain size*

161 A total of 84 surficial sediment samples (i.e., 44 limestone reef platform, 8 patch reef, 27 island and 5 offshore)
162 were collected (Figure. 1c). Standard wet sieving protocol and analysis was implemented to separate the samples
163 into seven sediment fractions (i.e., > 4000 µm, 2000 µm, 1000 µm, 500 µm and 250 µm, 125 µm and 63 µm)
164 (Syvitski, 2007; Cuttler et al., 2019). A Nikon SMZ445 stereo microscope (Nikon Metrology[®], Belgium) was
165 used to determine biogenic and siliciclastic composition of sediments from the 84 sample sites by identifying a
166 minimum of 100 grains per sieve fraction to a total of 500 grains per sample (Browne et al., 2013; Morgan and
167 Kench, 2016). The identification of sediments < 250 µm (the 125 µm and 63 µm fractions) was omitted from the
168 analysis due to the inability to accurately ascertain grain type due to samples being highly abraded. Sediments
169 were categorised into the following categories: coral, mollusc (i.e., gastropods and bivalves), crustose coralline
170 algae (CCA), foraminifera, echinoderm, bryozoan, *Halimeda*, siliciclastic (quartz), limestone fragments, other
171 carbonate and siliceous producers (i.e., crustaceans and coral/sponge spicules) or unknown. Biogenic sediments
172 that contributed more than 25% of the pooled sediment sample were categorised as '*x-rich*' in that constituent
173 (e.g. mollusc-rich or coral-rich).

174

175 *3.3 Reef ecology habitat survey*

176 *3.3.1 Limestone platform habitat*

177 The spatial coverage of modern benthic calcifying organisms was surveyed along two approximately 500 m
178 transects (see T1 & T2, Figure 3), stratified into a lower (western T2 transect) and higher (northern T1 transect)
179 wave energy site, as well as nearshore and offshore (distance from island landmass), including the: (1) inshore
180 limestone platform; (2) mid-intertidal limestone platform; and (3) offshore limestone platform. Seven quadrats (1
181 m²) were randomly placed in each zone (inner, middle, outer; Figure 2a) along each of the two transect lines (total

182 of $n = 21$ quadrats on each transect line) to determine relative benthic cover (%) in addition to benthic taxa
183 abundance. Percentage cover (%), based on area estimates, was recorded for the following categories: live reef-
184 building coral (sessile), crustose coralline algae (CCA), *Halimeda*, macro (fleshy brown and red algal species)
185 and turfing algae (multispecies algal assemblages <2 cm in height), sediment/rubble cover, and reef framework
186 rock (Tebbett & Bellwood, 2020; Dee et al., 2020). Abundance of benthic taxa including corals (grouped and
187 identified according to morphology), molluscs (minimum recorded size of ~2 cm), echinoids, bryozoans and
188 crustaceans were recorded (counted as individuals) in each quadrat. An additional 10 minute time count search
189 was conduct for molluscs around each quadrat.

190

191 3.3.2 Sub-reef habitat

192 Fourteen, 20 m shore parallel line transects were laid around Eva island's reef ranging between 1 and 4 m in depth
193 (Figure 3). Transects were stratified according to low (south – blue sample sites) and high (north – non-blue
194 sample sites) wave energy sites, to capture a diversity of benthic habitats (e.g. patch reef habitats, macroalgae and
195 bare bed/sandy bottom). Photographs were taken along each transect at two second intervals (< 1 m apart) on
196 SCUBA (approximately 0.5 m above the surface of the benthos), with a total of 60 photographs per transect. These
197 photographs (capturing approximately a 2 m² area) were used to quantify percent benthic cover (%) and abundance
198 using Coral Point Count software (CPCe v.3.6, Kohler and Gill 2006). To assess benthic cover, each photograph
199 was overlaid with 20 random points that were used to classify the benthos into the following categories: live coral
200 (sessile), crustose coralline algae (CCA), *Halimeda*, macro (fleshy brown and red algal species) and turfing algae
201 (multispecies algal assemblages <2 cm in height), sponge, sediment/rubble cover, and limestone rock (Tebbett &
202 Bellwood, 2020; Dee et al., 2020). Abundance (number of colonies or individuals) of benthic taxa including corals
203 (grouped and identified according to morphology), molluscs (minimum recorded size of ~2 cm) and echinoids
204 were recorded across each transect by counting individuals from each photograph and a 10 minute timed count
205 search along each 20 m transect (for molluscs and echinoids).

206

207 The photographic line transect method was used for the deeper sub-reef sites as this method is able to capture
208 larger areas of reef (meso-scale or larger) per unit of diving time when using SCUBA, as compared to conventional
209 quadrat surveys (Dumas et al., 2009). Therefore, to ensure estimates of percent cover were not under or over-
210 represented compared to the quadrat method using on the limestone platform, 1 m² quadrats were randomly laid

211 across selected transects and percent coral cover was quantified. When quadrat and photo transect methods were
212 compared, we found there to be < 2% difference.

213

214 3.4. Statistical analyses

215 Spatial interpolations of biogenic constituents (%) and grain size fractions (μm) were constructed using the
216 'kriging methods' function within SURFER[®] (v.10.1, GoldenSoftware[®], 2021) (Morgan and Kench, 2016b).
217 Agglomerative hierarchical cluster analysis was conducted in PAST[®] (PAleontological STatistics[®], v.2.17, 2021)
218 using the unweighted pair group method with arithmetic mean (UPGMA). Biosedimentary depositional facies
219 were identified using constructed Bray-Curtis similarity matrices (< 85% similarity) of square-root transformed
220 data on grain texture (percentage (%) of grain-size fractions, sorting) and relative contribution of biogenic skeletal
221 constituents (%) (Morgan and Kench, 2016b; Cuttler et al., 2019). Similarity percentage analysis (SIMPER) was
222 run to determine the primary factors driving (dis)similarity between biodepositional facies (Morgan and Kench,
223 2016b). Mann-Whitney *U*-tests (nonparametric rank-sum test) were conducted to discern statistical differences in
224 average grain size (μm) and sorting (σ) between reefal and island zones (Dawson and Smithers, 2010).

225

226 4. Results

227 4.1. Spatial distribution of ecological zones

228 Benthic habitat surveys identified four unique ecological zones at Eva Island, including: (1) limestone
229 platform, (2) live coral patch reef, (3) dead coral patch reef and (4) macroalgal bed (Figure 3i - v). Benthic cover
230 (%) across all offshore transects (Figure 3ii - v.) was dominated by macroalgae (primarily *Sargassium*, *Padina* &
231 *Dictyota sp.*, $49.8 \pm 11\%$) (Table 1). The live coral patch reef (Figure 3ii, -2 to -2.5 msl) at the northern periphery
232 of Eva exhibited highest percentage live coral cover (%), with mean (\pm standard deviation (SD)) live coral
233 accounting for $23 \pm 4.9\%$ of the reef surface and a high percentage sediment/rubble cover estimated at $13 \pm 5.6\%$.
234 Coral colonies identified consisted primarily of massive or submassive varieties of *Porites* (green and pink
235 morphotypes) and *Pavona sp.*, domal favids including *Favites* and *Dipsastrea sp.*, and a small abundance of
236 branching/tabulate *Acropora* and *Pocillopora sp.* Other calcifying taxa included non-geniculate CCA (primarily
237 *Porolithon sp.*, $3.3 \pm 3.1\%$). Mobile gastropods and bivalves were recorded in low abundance ($n = 12$ individuals)
238 (Table 1). The dead coral patch reef (Figure 3iii, -1.6 to -4 m msl) at the eastern periphery of the platform had low
239 hard coral cover ($11 \pm 4.9\%$) and the highest estimate of dead *in-situ* carbonate framework ($34 \pm 20.8\%$). At this
240 site, CCA (primarily *Porolithon sp.*) was a significant benthos component, recorded at $11 \pm 4.9\%$, with a similar

241 abundance of gastropods and bivalves ($n = 11$ individuals) as on the live coral patch reef (Table 1). Macroalgal
242 beds (Figure 3iv, -2 to -4.2 m msl) dominated both the southern (Figure 3iv) and western areas of the platform
243 (Figure 3v). The southern extent of Eva Island exhibited very low coverage of major sediment producers with
244 very low hard coral (4.1% on average) and CCA (1.8% on average) cover (Table 1). Similarly, the western
245 macroalgal zone had very low coral ($5.1 \pm 0.6\%$) and CCA ($3.2 \pm 4.5\%$) percent coverage, but the highest recorded
246 abundance of molluscs of all ecological zones ($n = 45$ individuals) (Table 1).

247 In contrast, the limestone platform (Figure 3i, -0.5 to -1.2 m msl) was a depositional environment with
248 high sediment coverage ($45.9 \pm 5.6\%$). Exposed limestone framework surface ($28.3 \pm 10.1\%$) provided substrate
249 for juvenile coral recruits ($3.7 \pm 0.4\%$, of 5 – 15 cm in diameter), CCA ($3.8 \pm 1.2\%$) and small green calcifying
250 algae of *Halimeda sp.* ($3.3 \pm 0.9\%$). This zone recorded the second highest abundance of molluscs ($n = 26$ total
251 individuals) (Table 1).

252

253 4.2. Sediment texture characteristics

254 Sand-sized material ($63\mu\text{m} - 2000\mu\text{m}$) contributed 72% (on average) of surficial sediments across reefal
255 sites, with silt-sized or smaller material ($< 63\mu\text{m}$) accounting for less than 3%. Highest proportion of gravel-sized
256 material ($> 2000\mu\text{m}$) occurred on the north-western platform (E8-NW) and decreased clockwise and anticlockwise
257 from this point around the circumference of the platform surface (Figure 4a & Figure 5a & b). No significant
258 shoreward trend in percentage gravel (i.e., decreasing % gravel with increasing distance from outer reef) was
259 observed ($R^2 = 0.02$, $F_{1, 54} = 1.47$, $p > 0.05$; Supplementary Figure I). Reefal sediment textures ranged from
260 medium sand ($315\mu\text{m}$) to fine gravel ($3570\mu\text{m}$), with a mean grain size of $1062 \mu\text{m}$ (very coarse sands) (Figure
261 4a). Sorting values were highly variable, and ranged from moderately well sorted (1.42σ) to very poorly sorted
262 (4.52σ), with a mean sorting of 2.25σ (poorly sorted) (Figure 4b). The largest sized and most poorly sorted
263 sediments were recorded on the windward north-west platform (Figure 4a – 4b).

264 Surficial island sediments were sand-sized dominated (97.5%, on average), with gravels and fines
265 accounting for less than 1.7% and 0.7%, respectively. Island sediments consisted of medium ($462\mu\text{m}$) to coarse
266 sand ($910\mu\text{m}$), with a mean grain size of $617\mu\text{m}$ (coarse sand) (Figure 4a). Sediment sorting ranged between well
267 sorted (1.37σ) and moderately sorted (1.72σ), with a mean sorting value of 1.58σ (moderately well sorted) (Figure
268 4b). Reefal and island sediments were texturally dissimilar, with significant differences in average grain size
269 (Mann-Whitney, $U = 272$, $Z = 3.87$, $p < 0.001$) and sorting (Mann-Whitney, $U = 164.5$, $Z = 5.65$, $p < 0.001$)

270 recorded between reef and island zones (Figure 4c – 4d). A trend in decreasing grain size is evident moving from
271 the NW side around the island.

272

273 4.3. Sediment assemblages

274 4.3.1 Reefal sediment skeletal composition

275 Mollusc (mean: $34 \pm 5.9\%$) and coral (mean: $31 \pm 8.9\%$) were the dominant skeletal constituents in reefal
276 sediments, contributing greatest to all size fractions (4000 μm to 250 μm). Concentration of molluscan constituents
277 (disarticulated gastropods and bivalves) were highest (up to 40%) on hard substrates on the western limestone
278 platform and the sandy southern sand bar (Figure 4f). Highest concentration of coral sediments (35-50%)
279 coincided with live coral reef framework and the carbonate reef platform located NNW of Eva Island (Figure 4e).
280 Areas of high coral-rich sediment (i.e., the coral framework patch reef and reef platform NNW of Eva Island
281 (Figure 4e & 4f.) corresponded with the lowest concentration of molluscs in the sediment ($< 30\%$, Figure 4e &
282 4f). CCA was also a prominent major sediment constituent (mean: $13 \pm 6.7\%$), and was shown to increase towards
283 the island shoreline (Figure 4g).

284 Remaining reef-derived sediments were generated by direct sediment producers including small benthic
285 foraminifera (mean: $5 \pm 1.7\%$) and echinoderms (mean: $4 \pm 3.6\%$). Both constituents were most abundant on the
286 outer reef platform and offshore reef environments to the west and north-east. Relict limestone (mean: $3 \pm 3.7\%$),
287 bryozoan (mean: $1 \pm 2.1\%$), siliciclastic (i.e. quartz, mean: $1 \pm 1.6\%$) and *Halimeda* spp. (mean: $0.3 \pm 0.3\%$)
288 material were not common in reefal sediments.

289

290 4.3.2 Island sediment skeletal composition

291 Sediment constituents were found to be homogenous across Eva Island, but was overall dominated by a
292 mix of mollusc (mean: $34 \pm 4.1\%$), coral (mean: $27 \pm 4.6\%$) and CCA (mean: $21 \pm 6.2\%$) across the sand/gravel
293 size fractions (4000 μm to 250 μm). Overall abundance of molluscan constituents (disarticulated gastropods and
294 bivalves) is consistent across island sediments (between 30-40%) with highest concentrations (35-40%) on the
295 north, north-east and south-east shorelines of Eva (Figure 4f). Similarly, coral-rich sediments (30-35%)
296 corresponded with areas of high mollusc (i.e., northern and south-east shoreline zones), and island
297 foredunes/vegetated swales and central island basin (Figure 4e). CCA constituents in island sediments were higher
298 (mean: $22 \pm 6.1\%$) than reefal zones, with greatest concentrations (15-30%) occurring on the island shoreline,

299 above foredunes/vegetated swales and basin (Figure 4g). Beach sediments on the north-west, south-east and
300 south-west of Eva exhibited highest contributions of CCA (> 25%, Figure 4g).

301 As per reefal zones, small benthic foraminifera and echinoids, on average, constituted $5 \pm 2.2\%$ and $4 \pm$
302 3.6% respectively. Relict limestone (mean: $2 \pm 3.1\%$), bryozoan (mean: $0.04 \pm 0.1\%$), siliciclastic (i.e. quartz, 0.7
303 $\pm 0.7\%$) and *Halimeda* spp. (mean: $0.04 \pm 0.1\%$) constituents were in very low abundances, with negligible
304 contribution to surficial island sediments.

305

306 *4.4. Biosedimentary depositional facies*

307 Depositional biosedimentary facies were identified based on hierarchal clustering (UPGMA by Bray-
308 Curtis < 85%) of composition and size fraction characteristics. Facies were distinguished by changes in sediment
309 grain size/texture and relative abundance of non-mollusc/coral skeletal fragments (i.e., rarer reef calcifies), with
310 a cumulative total pooled dissimilarity of 75% (derived from SIMPER statistical analyses).

311

312 Four biosedimentary facies were identified including: **(1)** Mollusc and coral-rich with echinoid &
313 foraminifera, moderately to poorly sorted medium sands (Cluster 1: offshore reef and, $n = 2$, mollusc: 35%, coral:
314 28%, echinoid & foraminifera: 9% respectively, Figure 6); **(2)** Mollusc-rich, mixed composition, moderately well
315 sorted to very poorly sorted coarse sands and fine gravels (Cluster 2: offshore bare bed, $n = 4$, mollusc: 37%,
316 coral: 20%, CCA: 10%, Figure 6.), **(3)** Coral & mollusc-rich with CCA, poorly sorted very coarse sands (Cluster
317 3: reef platform, sand bar, toe of beach, $n = 33$, coral: 34%, mollusc: 33%, CCA: 14%, Figure 6.); and **(4)** Mollusc
318 & coral-rich with CCA, moderately to moderately well sorted medium to coarse sands (Cluster 4: limestone
319 platform, island beach, vegetation zone, basin, $n = 45$, mollusc: 35%, coral: 28%, CCA: 18%, Figure 6).

320

321 **5. Discussion**

322

323 *5.1. Global comparison of reef island sediment constituents*

324

325 Surficial sediments from Eva Island and adjacent geomorphic environments (i.e., limestone platform and
326 patch reef habitats) are predominately composed of the skeletal remains of marine organisms, with mollusc
327 material (i.e., univalve gastropods and disarticulated bivalves) constituting 34% (on average) of reefal and 34%
328 (on average) of island sediments. The results of this study contrast with other Indo-Pacific and Caribbean reef
329 island systems, which have molluscs being a minor contributor to contemporary island sediments (Stoddart, 1962;

330 Folk & Robles, 1964; Woodroffe, 1992; Yamano et al., 2000; Kench et al., 2005; Dawson & Smithers, 2010;
331 Fuentes et al., 2010, McKoy et al., 2010). For example, at clear water localities including the Maldives (e.g.
332 Vabbinfaru, South Maalhosmadulu) and Iles Eparses (e.g. Glorieuses, Juan de Nova and Europa), within the
333 Indian Ocean, other constituents (e.g. coral, green algae (*Halimeda*), foraminifera) play a more dominant role
334 and represent a key long-term source of sediment (Woodroffe, 1992; Woodroffe et al., 1999; Kench et al., 2005;
335 Jorry et al., 2016; Morgan & Kench, 2016b). Throughout the central and western Pacific (e.g. Marshall Islands,
336 Green and Raine Island), benthic foraminifera are commonly the dominant sand-grade material, often exceeding
337 that of other reef calcifiers including corals, CCA and molluscs (Schofield, 1977; Dawson & Smithers, 2010;
338 Yamano et al., 2010; Fuentes et al., 2010; McKoy et al., 2010), whereas *Halimeda* constituents are dominant in
339 the Caribbean (Stoddart, 1962; Folk & Robles, 1964). One exception is Warraber Island in the Torres Strait, which
340 like Eva Island have molluscs representing a major contributor (54% on average) to island sediments (Hart &
341 Kench, 2007; Hart, 2008). A more detailed comparison is beyond the scope here, but below we discuss potential
342 reasons for the high proportion of mollusc-rich sediment at Eva Island in the Southern Pilbara of Western
343 Australia.

344

345 ***5.2. Eco-geomorphic disconnection between living mollusc abundance and mollusc-rich sediment*** 346 ***reservoir at Eva Island***

347

348 There is an observed inconsistency between the very low abundance of living molluscs ($n = 94$ individuals in ~
349 1700 m² of surveys) on Eva Island and the mass of mollusc-rich sediment (>500,000 m³ above msl) that forms the
350 island landmass. Few previous studies have also found a disconnection between the living ecological assemblages
351 and dominant sediment constituents (e.g. Molluscs: Hart & Kench, 2008; Coral: Cuttler et al., 2019). This
352 observation is interesting, given that the preferred habitat requirements by extant molluscs, which include
353 consolidated limestone reef pavement, pockets or veneering carbonate sediments, minor live coral cover and
354 spatially expansive and diverse macro and/or turf algae (Slack-Smith & Bryce, 2004; Floyd et al., 2020; Nagai et
355 al., 2011), are present at Eva Island and adjacent nearshore island localities. Here, we discuss a combination of
356 geo-physical and ecological processes that might explain this disparity, presenting four plausible hypotheses:

357

358 ***1. Influence of life span/cycle and turnover rates***

359 High abundance of molluscs in the detrital assemblage may be the direct consequence of the biota's short life
360 spans. Existing knowledge from the literature on mollusc life histories, particularly their life span is scarce
361 (Albano and Sabelli, 2011). Several studies have indicated molluscs to exhibit multi-year life spans (i.e., between
362 4 – 7 years). In neighbouring Ningaloo Reef Marine Park, species (e.g. gastropods) have been estimated to live
363 for several years, with few exhibiting annual life cycles (Black et al., 2011). Research by Albano and Sabelli
364 (2011) postulated that skeletal remains of molluscs with short life spans (i.e., herbivorous molluscs) are more
365 frequently added to the death assemblage compared to their carnivorous counterparts, and therefore are more
366 abundant as dominant sediment constituents. Considering this, low recorded abundances in the living assemblage
367 on Eva may have been a direct consequence of surveying at the end of a multi-year life-cycle, further confounded
368 by underestimation of abundance due to the often cryptic and/or nocturnal behaviour of many molluscs (Riegl et
369 al., 2008; Netchy et al., 2016). It can also be postulated that these extant populations are of the herbivorous variety
370 as the presence of macroalgal beds and in general high macroalgae cover, are shown to support grazing by meso-
371 and macroinvertebrate herbivores including molluscs (Harrison and Booth, 2007). Yet, validating this hypothesis
372 is dependent on understanding species and/or population specific life-cycle dynamics, behaviours and turnover
373 rates, which by this criterion, requires continued rigorous monitoring (e.g. monthly per year over several years)
374 to resolve this unknown (Black et al., 2011).

375

376 **2. Immediate contribution to detrital assemblage and short residence time**

377 Abundance of living sediment producers may not directly relate to sediment composition, but instead, may reflect
378 differential skeletal durability and hence residence times (Liang et al., 2016). The high durability and low settling
379 velocity of molluscs allow for them to be readily retained in the sediment, in addition to broken-down into
380 transportable sized material, whereas other calcifiers such as coral/CCA take longer to breakdown within the
381 system (Hart, 2008; Ford & Kench, 2012). Further, the immediate contribution of the organism to the detrital
382 sediment reservoir on death in addition to the mollusc component consisting predominantly of disarticulated shell
383 (i.e., gastropod and bivalve) fragments may also partly explain the high abundance in both platform and island
384 beach sediments despite low numbers in the living assemblage. This contrasts with coral and CCA that require an
385 additional step of skeletal breakdown (e.g. mechanical and/or biological erosion) in addition to lower turnover
386 rates (Chave, 1964; Force, 1969; Kench and McLean, 1996; Hart and Kench, 2008). Once deposited on the
387 shoreline, molluscan constituents may be further winnowed by aeolian (wind driven) processes – transported and
388 incorporated into the island landmass. Together, these factors could explain compositional similarities between

389 reefal and island sediments, suggesting there is an active sedimentary connection between reef (source) and island
390 (sink) (i.e., whereby modern and/or relict sediments are being supplied to the island), despite depauperate numbers
391 of living molluscs in the contemporary reef ecological assemblage.

392

393 **3. *Temporal changes in community composition***

394 Records of environmental change may have caused significant, yet unreported, variations in mollusc community
395 assemblages in the region. In recent years, changes in regimes of environmental conditions and acute disturbance
396 events (e.g. Marine Heat Waves (MHWs)) are more pronounced in marginal ecosystems such as turbid coral reefs.
397 A study by Smale et al., (2017) following the 2010/2011 MHW event off Western Australia, showed that mollusc
398 populations exhibited increased susceptibility to prolonged and extreme temperatures (+ 2°C and + 3°C
399 temperature anomalies respectively, persisting over 2 months), inducing deleterious physiological responses and
400 high mortality rates, which resulted in extensive die-off events. Since 2010/2011, three strong thermal anomaly
401 events (exceeding 14° heating weeks (DHW)) occurred in coastal waters off the Pilbara, Western Australia, during
402 two Austral summers (i.e. 2010/2011; 2013/2014), causing prolonged and elevated SSTs (Evans et al., 2020;
403 Babcock et al., 2021). It is possible that the direct response to increased SSTs by the 2010 – 2014 MHWs could
404 have induced significant die-off in mollusc assemblages regionally, including on Eva’s platform and surrounding
405 reef habitats, resulting in a depauperate extant population. Recovery of mollusc populations may be further
406 hampered by either (1) reduced proximity to source populations, where the sources are likely from higher latitudes
407 from which larvae do not survive dispersal to the region (of short lifespans) or (2) lack of connectivity between
408 local sources (e.g. Ningaloo Reef) and the Exmouth Gulf due to weak ocean circulation in these nearshore reef
409 environments (Feng et al., 2016; Doropoulos et al., 2022). The combination of high skeletal durability, high
410 turnover rates and a potential die-off event may have led to a pulse of mollusc-dominated sediment within the
411 sediment reservoir, which has then been followed by a hiatus in mollusc sediment production.

412

413 **4. *External sources of sediment supply***

414 Mollusc-rich sediments may be allochthonous - generated at distal offshore locations, from which they may be
415 directly transported and deposited into the local system overtime via high-energy pulse events (i.e., cyclones,
416 surge, and storms). *In-situ* observational evidence by Dufois et al., (2017) has suggested that alongshore
417 propagation of tropical cyclones (TCs) across the North West Shelf (NWS) of Australia have been responsible for
418 generating high sediment resuspension and south-westward sediment transport, particularly towards the southern

419 extent of the NWS (towards Exmouth Gulf). Numerical modelling of the activity of 19 tropical cyclones (spanning
420 14 years) over the NWS further supports this case, confirming that TCs drive the majority of alongshore and
421 seaward sediment transport over most of the shelf (Dufois et al., 2018). Considering this, the south-westward
422 circulation pattern across the region suggest that sediments may have originated farther north of Eva Island (e.g.
423 the northern NWS), transported to the island system by pulse events generated by tropical cyclone activity, from
424 which they are supplied to the island via local hydrodynamic processes.

425

426 *5.3 Implications for reef island resilience*

427

428 Coral reefs and reef-associated landforms are highly sensitive to the impacts of environmental
429 change (Perry et al., 2011; Bonesso et al., 2017; Hughes et al., 2017; Browne et al., 2021). Climate change
430 related shifts in SSTs, ocean chemistry and storm frequency/intensity directly impact coral reef organisms
431 (and thus reef-derived sediments), which may alter the ecological state of a system and its overall carbonate
432 sediment budget (Perry et al., 2011; Cuttler et al., 2019, Browne et al., 2021). Whilst an observed
433 disconnection between living ecological assemblage and sediment constituents exists at Eva, relative
434 homogeneity between biosedimentary facies reinforce a coupling between reef (source) and island (sink)
435 environments, indicating that there is an active exchange of sediment being supplied to the island landform.
436 If sediment generation processes on the surrounding reefs are maintained at current (or higher) levels, the
437 active sediment exchange between reef and island suggests that the landform may be currently resilient to
438 extrinsic impacts such as sea level rise.

439 Yet, it is likely that rates of sediment generation will be negatively influenced with future climate
440 change, although the extent of a decline in sediment sources will depend on the contemporary key drivers and
441 processes of sediment production/supply. Here we found a disconnection between the living mollusc
442 assemblage, which was low in abundance ($n = 94$ individuals), and the sediment composition, which was
443 characterised by high proportion of molluscan fragments. We hypothesised that this disconnection was due
444 to either; (1) natural life cycles/turnover rates, (2) skeletal durability and short residence times, (3) acute
445 environmental disturbance events (MHWs) and, (4) distal offshore sediment supply (alongshore transport
446 across the NWS). In the case where disconnection between living assemblage and sediment constituents is
447 the result of an external sediment supply (Hypothesis 4) versus locally generated (Hypothesis 2), this may
448 support island maintenance (and resilience) as it reduces reliance on a smaller (local) and, therefore, more

449 vulnerable sediment source. Alternatively, if this disconnection is due to natural biological processes such as
450 life cycle/turnover rates (Hypothesis 1) in place of an acute disturbance event (e.g. MHWs) (Hypothesis 3),
451 this would suggest that mollusc assemblages either rapidly recovered or were not heavily impacted by the
452 two recent MHW's, and that Eva's mollusc population enhance island resilience to future climate change
453 conditions. In contrast, a die off following a marine heatwave could compromise long-term resilience due to
454 an immediate decline in sediment producers, despite immediate contribution to the detrital sediment reservoir.
455 To improve current evaluation of island resilience, and determine which (or combination) of these hypothesis
456 may be influencing mollusc populations, further work would be needed including dating of sediment samples
457 (to discern whether modern and/or relict), sediment tracking, and conducting an intensive sediment sampling
458 programme.

459
460 Whilst molluscs are a dominant sediment constituent of Eva Island's sediment reservoir, equal
461 proportions of coral and to a lesser amount CCA, are shown to make up the bulk remainder of the sediment
462 material (~ 40-50% on average). Thus, changes in the production and supply dynamics of any of these
463 sediment constituents could impact island nourishment and development. However, this may be particularly
464 acute where the dominant biogenic contributors to reef island nourishment are sensitive to the same
465 environmental impacts (i.e., marine heat waves). Therefore, long-term island resilience may be compromised
466 with future environmental perturbations, where the sensitivity of islands is influenced by changes in sediment
467 producing habitats and thus a direct impact on the organisms which occupy these habitats overtime. Islands
468 composed of several constituent components are likely to exhibit increased resilience to environmental
469 changes, compared to islands that are comprised of only one dominant primary component. Here we found
470 that Eva has a comparatively diverse sediment composition (i.e. equal proportion of mollusc and coral) to
471 other reef islands, which have been shown to be dominated by a single component (e.g. coral or foraminifera).
472 This would suggest that Eva has greater potential resilience when compared to islands with less diverse
473 sediment assemblages. Despite more diverse sediment assemblages, sediment production rates may still be
474 negatively influenced by future perturbations in environmental change, but the rate of decline will potentially
475 be slower than if its sediment budget was largely reliant on a single component.

476

477 **6. Conclusion**

478 This study presents the first regional measurement of sediment composition of an inshore turbid reef
479 island from the eastern Indian Ocean and provides *in-situ* evidence that molluscs are a dominant constituent of
480 both reefal and island sediments, despite recorded low abundances in the reef ecology of Eva Island. We propose
481 four hypotheses to explain this disparity. However, it is unlikely that a single hypothesis can account for this
482 inconsistency, and this may be a function of several interacting factors across broad spatial and temporal
483 timescales. Despite this, a visible coupling between source (reef) and sink (island) environments may exist, with
484 the sediment reservoir actively supplying available material for island nourishment. This is further supported by
485 the relative homogeneity within the biosedimentary facies, reinforcing the similarity in source sediments between
486 reef and island. Future validation of sediment age will be imperative to determine whether material is modern or
487 relict. In light of these findings, assuming that island building processes can keep up with sea level rise (SLR),
488 Eva is likely to be resilient, unless dominant sediment constituents change or there is a decline in critical sediment
489 producers (molluscs and coral) following future perturbations in environmental change.

490

491 **Declaration of competing interest**

492 The authors declare that they have no competing financial or intellectual interests that could have influenced the
493 work reported in this publication.

494

495 **Acknowledgments**

496 This project was funded by an Australian Research Council (ARC) DECRA Fellowship
497 DE180100391 awarded to Dr Nicola Browne of Curtin University of Technology, Perth, as part of the island
498 resilience project (2018–2020). The authors would like to extend their thanks to Adi Zveifler, Jennifer McIlwain,
499 Kesia Savil and Jake Neilsen for field support and logistical assistance. We would also like to acknowledge the
500 Minderoo Foundation for their support with assistance in the field, in particular boating operations and equipment
501 logistics. Special thanks to Michael Tropiano and Nikki DeCampe. The authors would also like to acknowledge
502 the support and expertise of Dr Jane Prince and Dr Renae Hovey for their invaluable advice on invertebrate
503 ecological survey methodology and identification training. Lastly, we thank Professor Simon Lang and Associate
504 Professor Nik Callow for providing access to the drone for acquiring the aerial photographs presented in this
505 paper.

506

507

508

509

510 **References**

511

512 Albano, P.G., Sabelli, B., 2011. Comparison between death and living molluscs assemblages in a Mediterranean
513 infralittoral off-shore reef. *Palaeogeography, Palaeoclimatology, Palaeoecology* 310, 206-215.

514 Babcock, R.C., Thomson, D.P., Haywood, M.D.E., Vanderklift, M.A., Pillans, R., Rochester, W.A., Miller, M.,
515 Speed, C.W., Shedrawi, G., Field, S., 2020. Recurrent coral bleaching in north-western Australia and
516 associated declines in coral cover. *Marine and Freshwater Research* 72, 620-632.

517 Black, R., Johnson, M.S., Prince, J., Brearley, A., 2011. WAMSI 3.2.2b final report: Diversity, abundance and
518 distribution of intertidal invertebrate species in the Ningaloo Marine Park (Technical Report). Western
519 Australian Marine Science Institution, 452 pp.

520 Bonesso, J.L., Cuttler, M.V.W., Browne, N., Hacker, J., O'Leary, M., 2020. Assessing Reef Island Sensitivity
521 Based on LiDAR-Derived Morphometric Indicators. *Remote Sensing* 12, 3033.

522 Bonesso, J.L., Leggat, W., Ainsworth, T.D., 2017. Exposure to elevated sea-surface temperatures below the
523 bleaching threshold impairs coral recovery and regeneration following injury. *PeerJ* 5, e3719.

524 Browne, N., Braoun, C., McIlwain, J., Nagarajan, R., Zinke, J., 2019. Borneo coral reefs subject to high sediment
525 loads show evidence of resilience to various environmental stressors. *PeerJ* 7, e7382.

526 Browne, N.K., Cuttler, M., Moon, K., Morgan, K., Ross, C.L., Castro-Sanguino, C., Kennedy, E., Harris, D.,
527 Barnes, P., Bauman, A., 2021. Predicting responses of geo-ecological carbonate reef systems to climate
528 change: a conceptual model and review. *Oceanography and Marine Biology: An Annual Review*,
529 Volume 59 59, 229-370.

530 Browne, N.K., Smithers, S.G., Perry, C.T., 2013. Carbonate and terrigenous sediment budgets for two inshore
531 turbid reefs on the central Great Barrier Reef. *Marine Geology* 346, 101-123.

532 Cartwright, P.J., Fearn, P.R.C.S., Branson, P., Cutler, M.V.W., O'leary, M., Browne, N.K., Lowe, R.J., 2021.
533 Identifying Metocean Drivers of Turbidity Using 18 Years of MODIS Satellite Data: Implications for
534 Marine Ecosystems under Climate Change. *Remote Sensing* 13, 3616.

535 Cassata, L., Collins, L.B., 2008. Coral reef communities, habitats, and substrates in and near sanctuary zones of
536 Ningaloo Marine Park. *Journal of Coastal Research* 24, 139-151.

537 Chave, K.E., 1964. Skeletal durability and preservation. *Approaches to paleoecology*.

538 Cuttler, M.V., Hansen, J.E., Lowe, R.J., Trotter, J.A., McCulloch, M.T., 2019. Source and supply of sediment to
539 a shoreline salient in a fringing reef environment. *Earth Surface Processes and Landforms* 44, 552-564.

540 Cuttler, M.V.W., Vos, K., Branson, P., Hansen, J.E., O'leary, M., Browne, N.K., Lowe, R.J., 2020. Interannual
541 response of reef islands to climate-driven variations in water level and wave climate. *Remote Sensing*
542 12, 4089.

543 Dawson, J.L., Hua, Q., Smithers, S., Benthic foraminifera: their importance to future reef island resilience. In,
544 12th International Coral Reef Symposium, Cairns, QLD, Australia. Abstract retrieved from [http://www.](http://www.icsr2012.com/proceedings/manuscripts/ICRS2012_1A_1)
545 [icsr2012.com/proceedings/manuscripts/ICRS2012_1A_1](http://www.icsr2012.com/proceedings/manuscripts/ICRS2012_1A_1). Pdf. 2012, International Coral Reef Society.

546 Dawson, J.L., Smithers, S.G., 2010. Shoreline and beach volume change between 1967 and 2007 at Raine Island,
547 Great Barrier Reef, Australia. *Global and Planetary Change* 72, 141-154.

548 Dawson, J.L., Smithers, S.G., 2014. Carbonate sediment production, transport, and supply to a coral cay at Raine
549 Reef, Northern Great Barrier Reef, Australia: a facies approach. *Journal of Sedimentary Research* 84,
550 1120-1138.

551 Dee, S., Cuttler, M., Cartwright, P., McIlwain, J., Browne, N., 2021. Encrusters maintain stable carbonate
552 production despite temperature anomalies among two inshore island reefs of the Pilbara, Western
553 Australia. *Marine Environmental Research*, 105386.

554 Dee, S., Cuttler, M., O'Leary, M., Hacker, J., Browne, N., 2020. The complexity of calculating an accurate
555 carbonate budget. *Coral Reefs*, 1-10.

556 Dufois, F., Lowe, R.J., Branson, P., Fearn, P., 2017. Tropical Cyclone- Driven Sediment Dynamics Over the
557 Australian North West Shelf. *Journal of Geophysical Research: Oceans* 122, 10225-10244.

558 Dufois, F., Lowe, R.J., Rayson, M.D., Branson, P.M., 2018. A Numerical Study of Tropical Cyclone- Induced
559 Sediment Dynamics on the Australian North West Shelf. *Journal of Geophysical Research: Oceans* 123,
560 5113-5133.

561 Dumas, P., Bertaud, A., Peignon, C., Leopold, M., Pelletier, D., 2009. A "quick and clean" photographic method
562 for the description of coral reef habitats. *Journal of Experimental Marine Biology and Ecology* 368, 161-
563 168.

564 East, H., Perry, C., Kench, P., Liang, Y., Gulliver, P., 2018. Coral reef island initiation and development under
565 higher than present sea levels. *Geophysical Research Letters* 45, 11,265-211,274.

566 Evans, R.D., Wilson, S.K., Fisher, R., Ryan, N.M., Babcock, R., Blakeway, D., Bond, T., Dotji, P., Dufois, F.,
567 Fearn, P., 2020. Early recovery dynamics of turbid coral reefs after recurring bleaching events. *Journal*
568 *of Environmental Management* 268, 110666.

569 Floyd, M., Mizuyama, M., Obuchi, M., Sommer, B., Miller, M.G.R., Kawamura, I., Kise, H., Reimer, J.D., Beger,
570 M., 2020. Functional diversity of reef molluscs along a tropical-to-temperate gradient. *Coral Reefs* 39,
571 1361-1376.

572 Folk, R.L., Robles, R., 1964. Carbonate sands of isla perez, alacran reef complex, Yucatan. *The Journal of*
573 *Geology* 72, 255-292.

574 Force, L.M., 1969. Calcium carbonate size distribution on the west Florida shelf and experimental studies on the
575 microarchitectural control of skeletal breakdown. *Journal of Sedimentary Research* 39, 902-934.

576 Ford, M.R., Kench, P.S., 2012. The durability of bioclastic sediments and implications for coral reef deposit
577 formation. *Sedimentology* 59, 830-842.

578 Ford, M.R., Kench, P.S., 2015. Multi-decadal shoreline changes in response to sea level rise in the Marshall
579 Islands. *Anthropocene* 11, 14-24.

580 Ford, M.R., Kench, P.S., 2016. Spatiotemporal variability of typhoon impacts and relaxation intervals on Jaluit
581 Atoll, Marshall Islands. *Geology* 44, 159-162.

582 Ford, M.R., Kench, P.S., Owen, S.D., Hua, Q., 2020. Active sediment generation on coral reef flats contributes to
583 recent reef island expansion. *Geophysical Research Letters* 47, e2020GL088752.

584 Fossette, S., Ferreira, L.C., Whiting, S.D., King, J., Pendoley, K., Shimada, T., Speirs, M., Tucker, A.D., Wilson,
585 P., Thums, M., 2021. Movements and distribution of hawksbill turtles in the Eastern Indian Ocean.
586 *Global Ecology and Conservation* 29, e01713.

587 Fuentes, M., Dawson, J., Smithers, S., Hamann, M., Limpus, C., 2010. Sedimentological characteristics of key
588 sea turtle rookeries: potential implications under projected climate change. *Marine and Freshwater*
589 *Research* 61, 464-473.

590 Harney, J.N., Fletcher Iii, C.H., 2003. A budget of carbonate framework and sediment production, Kailua Bay,
591 Oahu, Hawaii. *Journal of Sedimentary Research* 73, 856-868.

592 Harney, J.N., Grossman, E.E., Richmond, B.M., Fletcher Iii, C.H., 2000. Age and composition of carbonate
593 shoreface sediments, Kailua Bay, Oahu, Hawaii. *Coral reefs* 19, 141-154.

594 Harris, D.L., Rovere, A., Casella, E., Power, H., Canavesio, R., Collin, A., Pomeroy, A., Webster, J.M.,
595 Parravicini, V., 2018. Coral reef structural complexity provides important coastal protection from waves
596 under rising sea levels. *Science advances* 4, eaao4350.

597 Harrison, P.L., Booth, D.J., 2007. Coral reefs: naturally dynamic and increasingly disturbed ecosystems. *Marine*
598 *ecology*, 316-377.

599 Hart, D.E., The maintenance of reef islands. In, *Proc 11th Int Coral Reef Symp.* 2008, pp. 416-420.

600 Hart, D.E., Kench, P.S., 2007. Carbonate production of an emergent reef platform, Warraber Island, Torres Strait,
601 Australia. *Coral Reefs* 26, 53-68.

602 Hughes, T.P., Kerry, J.T., Álvarez-Noriega, M., Álvarez-Romero, J.G., Anderson, K.D., Baird, A.H., Babcock,
603 R.C., Bejer, M., Bellwood, D.R., Berkemans, R., 2017. Global warming and recurrent mass bleaching
604 of corals. *Nature* 543, 373-377.

605 Jorry, S.J., Camoin, G.F., Jouet, G., Le Roy, P., Vella, C., Courgeon, S., Prat, S., Fontanier, C., Paumard, V.,
606 Boule, J., 2016. Modern sediments and Pleistocene reefs from isolated carbonate platforms (Iles Eparses,
607 SW Indian Ocean): a preliminary study. *Acta oecologica* 72, 129-143.

608 Kench, P., Parnell, K., Brander, R., 2003. A process based assessment of engineered structures on reef islands of
609 the Maldives.

610 Kench, P.S., McLean, R.F., 1996. Hydraulic characteristics of bioclastic deposits: new possibilities for
611 environmental interpretation using settling velocity fractions. *Sedimentology* 43, 561-570.

612 Kench, P.S., McLean, R.F., 2004. Hydrodynamics and sediment flux of hoas in an Indian Ocean atoll. *Earth Surface*
613 *Processes and Landforms: The Journal of the British Geomorphological Research Group* 29, 933-953.

614 Kench, P.S., McLean, R.F., Nichol, S.L., 2005. New model of reef-island evolution: Maldives, Indian Ocean.
615 *Geology* 33, 145-148.

616 Kohler, K.E., Gill, S.M., 2006. Coral Point Count with Excel extensions (CPCe): A Visual Basic program for the
617 determination of coral and substrate coverage using random point count methodology. *Computers &*
618 *geosciences* 32, 1259-1269.

619 Liang, Y., Kench, P.S., Ford, M.R., East, H.K., 2016. Lagoonal reef sediment supply and island connectivity,
620 Huvadhu Atoll, Maldives. *Journal of Coastal Research*, 587-591.

621 McKoy, H., Kennedy, D.M., Kench, P.S., 2010. Sand cay evolution on reef platforms, Mamanuca Islands, Fiji.
622 *Marine Geology* 269, 61-73.

623 McLean, R., Kench, P., 2015. Destruction or persistence of coral atoll islands in the face of 20th and 21st century
624 sea- level rise? *Wiley Interdisciplinary Reviews: Climate Change* 6, 445-463.

625 Morgan, K.M., Kench, P.S., 2014. A detrital sediment budget of a Maldivian reef platform. *Geomorphology* 222,
626 122-131.

627 Morgan, K.M., Kench, P.S., 2016a. Parrotfish erosion underpins reef growth, sand talus development and island
628 building in the Maldives. *Sedimentary geology* 341, 50-57.

629 Morgan, K.M., Kench, P.S., 2016b. Reef to island sediment connections on a Maldivian carbonate platform: using
630 benthic ecology and biosedimentary depositional facies to examine island- building potential. *Earth*
631 *Surface Processes and Landforms* 41, 1815-1825.

632 Morgan, K.M., Perry, C.T., Johnson, J.A., Smithers, S.G., 2017. Nearshore turbid-zone corals exhibit high
633 bleaching tolerance on the Great Barrier Reef following the 2016 ocean warming event. *Frontiers in*
634 *Marine Science* 4, 224.

635 Muir, P.R., Wallace, C.C., Done, T., Aguirre, J.D., 2015. Limited scope for latitudinal extension of reef corals.
636 *Science* 348, 1135-1138.

637 Netchy, K., Hallock, P., Lunz, K.S., Daly, K.L., 2016. Epibenthic mobile invertebrate diversity organized by coral
638 habitat in Florida. *Marine Biodiversity* 46, 451-463.

639 Nott, J., Hubbert, G., 2005. Comparisons between topographically surveyed debris lines and modelled inundation
640 levels from severe tropical cyclones Vance and Chris, and their geomorphic impact on the sand coast.
641 *Australian Meteorological Magazine* 54, 187-196.

642 Perry, C.T., Kench, P.S., O'Leary, M., Morgan, K., Januchowski-Hartley, F., 2015. Linking reef ecology to island
643 building: Parrotfish identified as major producers of island-building sediment in the Maldives. *Geology*
644 43, 503-506.

645 Perry, C.T., Kench, P.S., Smithers, S.G., Riegl, B., Yamano, H., O'Leary, M.J., 2011. Implications of reef
646 ecosystem change for the stability and maintenance of coral reef islands. *Global Change Biology* 17,
647 3679-3696.

648 Perry, C.T., Kench, P.S., Smithers, S.G., Yamano, H., O'Leary, M., Gulliver, P., 2013. Time scales and modes of
649 reef lagoon infilling in the Maldives and controls on the onset of reef island formation. *Geology* 41,
650 1111-1114.

651 Riegl, B.M., Dodge, R.E., 2008. *Coral Reefs of the USA*, 1. Springer Science & Business Media.

652 Schofield, J.C., 1977. Effect of Late Holocene sea-level fall on atoll development. *New Zealand Journal of*
653 *Geology and Geophysics* 20, 531-536.

654 Slack-Smith, S.M., Bryce, C.W., 2004. A survey of the benthic molluscs of the Dampier Archipelago, Western
655 Australia. *Records of the Western Australian Museum Supplement* 66, 221-245.

656 Smale, D.A., Wernberg, T., Vanderklift, M.A., 2017. Regional-scale variability in the response of benthic
657 macroinvertebrate assemblages to a marine heatwave. *Marine Ecology Progress Series* 568, 17-30.

658 Smithers, S.G., 1994. Sediment facies of the Cocos (Keeling) islands. *Atoll Research Bulletin*.

659 Sommer, B., Beger, M., Harrison, P.L., Babcock, R.C., Pandolfi, J.M., 2018. Differential response to abiotic stress
660 controls species distributions at biogeographic transition zones. *Ecography* 41, 478-490.

661 Sorby, H.C., 1879. The structure and origin of limestones. *The Popular science review* 3, 134-137.

662 Stoddart, D.R., 1962. Three Caribbean atolls: Turneffe Islands, Lighthouse Reef, and Glover's Reef, British
663 Honduras. *Atoll Research Bulletin*.

664 Sully, S., van Woesik, R., 2020. Turbid reefs moderate coral bleaching under climate- related temperature stress.
665 *Global Change Biology* 26, 1367-1373.

666 Tebbett, S.B., Bellwood, D.R., 2019. Algal turf sediments on coral reefs: what's known and what's next. *Marine*
667 *pollution bulletin* 149, 110542.

668 Twigg, E.J., Collins, L.B., 2010. Development and demise of a fringing coral reef during Holocene
669 environmental change, eastern Ningaloo Reef, Western Australia. *Marine Geology* 275, 20-36.

670 Webb, A.P., Kench, P.S., 2010. The dynamic response of reef islands to sea-level rise: evidence from multi-
671 decadal analysis of island change in the Central Pacific. *Global and Planetary Change* 72, 234-246.

672 Woodroffe, C.D., McLean, R., 1992. Kiribati vulnerability to accelerated sea-level rise: a preliminary study.

673 Woodroffe, C.D., McLean, R.F., Smithers, S.G., Lawson, E.M., 1999. Atoll reef-island formation and response
674 to sea-level change: West Island, Cocos (Keeling) Islands. *Marine Geology* 160, 85-104.

675 Yamano, H., Kayanne, H., Chikamori, M., 2005. An overview of the nature and dynamics of reef islands. *Global*
676 *Environmental research - English Edition* - 9, 9.

677 Yamano, H., Kayanne, H., Yamaguchi, T., Kuwahara, Y., Yokoki, H., Shimazaki, H., Chikamori, M., 2007. Atoll
678 island vulnerability to flooding and inundation revealed by historical reconstruction: Fongafale Islet,
679 Funafuti Atoll, Tuvalu. *Global and Planetary Change* 57, 407-416.

680 Yamano, H., Miyajima, T., Koike, I., 2000. Importance of foraminifera for the formation and maintenance of a
681 coral sand cay: Green Island, Australia. *Coral Reefs* 19, 51-58.

682
683
684
685
686
687
688
689
690
691
692
693
694
695
696
697
698
699
700
701
702
703
704
705
706
707
708
709
710
711

Figure captions

(Please note: colour will need to be used for all figures in final print)

Figure 1. Location of (a) Eva Island (highlighted in yellow), and neighbouring islands in the Exmouth Gulf; (b) location of Exmouth Gulf Region in Western Australia and; (c) sediment collection sites used for grain size and compositional analysis (**black dots**) overlain on raw airborne-bathymetric LiDAR DEM of Eva Island (0.5 m resolution) and its surrounding sub-reef systems (0.1 m resolution). No airborne-bathymetric LiDAR for offshore regions are currently available and were hence absent from the DEM image.

Figure 2. Geomorphological observations at Eva Island showing (a) aerial view of island features and neighbouring Y Island in distance, (b) beachrock pavement at the northern periphery of island landmass, (c) scarpred foredune (with coastal endemic spinifex grass), (d) sub-tidal patch reef exhibiting live and dead *in-situ* framework and (e) aerial view of sandy spit, toe of beach, vegetated swales and vegetation line.

Figure 3. Ecological zones identified on Eva Island. Shaded regions of charts represent mean percent (%) benthic cover (AL, Macro and Turfing Algae; L/DC, Limestone/dead *in-situ* coral; SED, Sediment; LC, Live Coral; CCA, Crustose Coralline Algae; HAL, *Halimeda*; SP, Sponge. Zones (i – v) represent habitat characteristics for each identified ecological zone. Coloured images (and associated pie charts labelled i - v) represent each ecological zone (coloured dots) as shown on the airborne-bathymetric DEM of Eva Island.

Figure 4. Spatial interpolation maps of sediment texture characteristics including: (a) mean grain size (μm) and, (b) sorting values (σ); (c & d) box and whisker plots of average grain size (μm) and sorting (σ). Relative (%) contribution of skeletal and siliciclastic constituents in surface sediments including (e) Coral; (f) Mollusc; and, (g) CCA remains. Krigged surfaces are clipped to the spatial extent of the benthic sediment samples.

Figure 5. The (a) **inferred gravel** movement (direction denote by arrows) corresponding to (b) change in the proportion of gravel in surficial sediments (%) across each transect (transect identified by colour shading). Inferred movement of sediment is roughly circular around the periphery of the island landmass.

712 **Figure 6.** Spatial distribution of biosedimentary facies at Eva Island as identified through agglomerative
713 hierarchal cluster analysis. Shaded regions of charts denote percentage contribution of coral (C), mollusc (M),
714 Crustose Coralline Algae (CCA), Foraminifera (F), Echinoderms (E), Bryozoans (BRY), limestone (L), other
715 califiers (O), siliciclastic (S), unknown (U) and *Halimeda* (H).

716

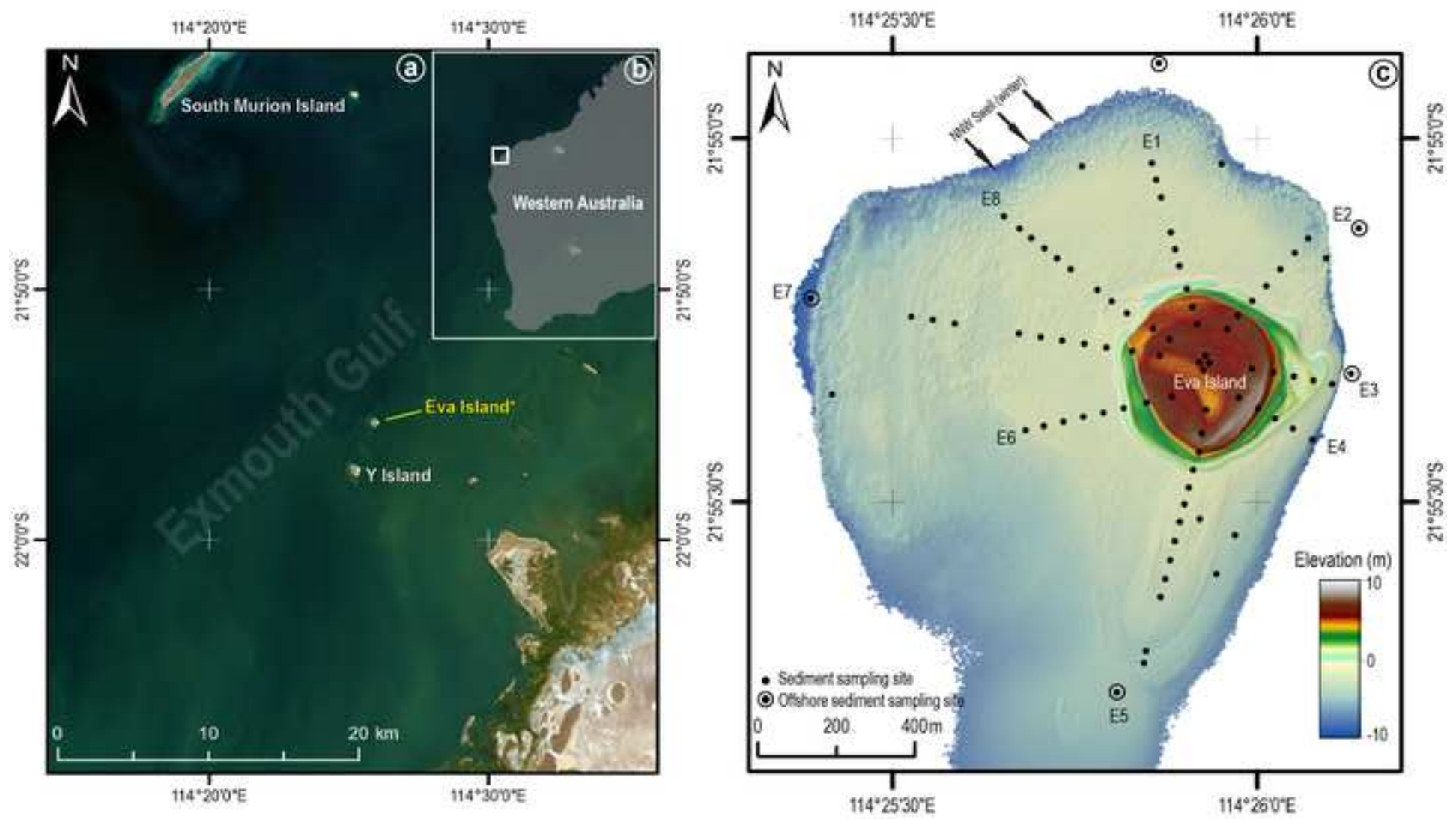
717 **Table 1.** Ecological zones are derived from benthic habitat surveys of Eva Island and Reef. Mean \pm SD are
718 presented for benthic cover across all zones.

719

720

Figure 1.

[Click here to access/download;Figure;Figure 1.png](#)



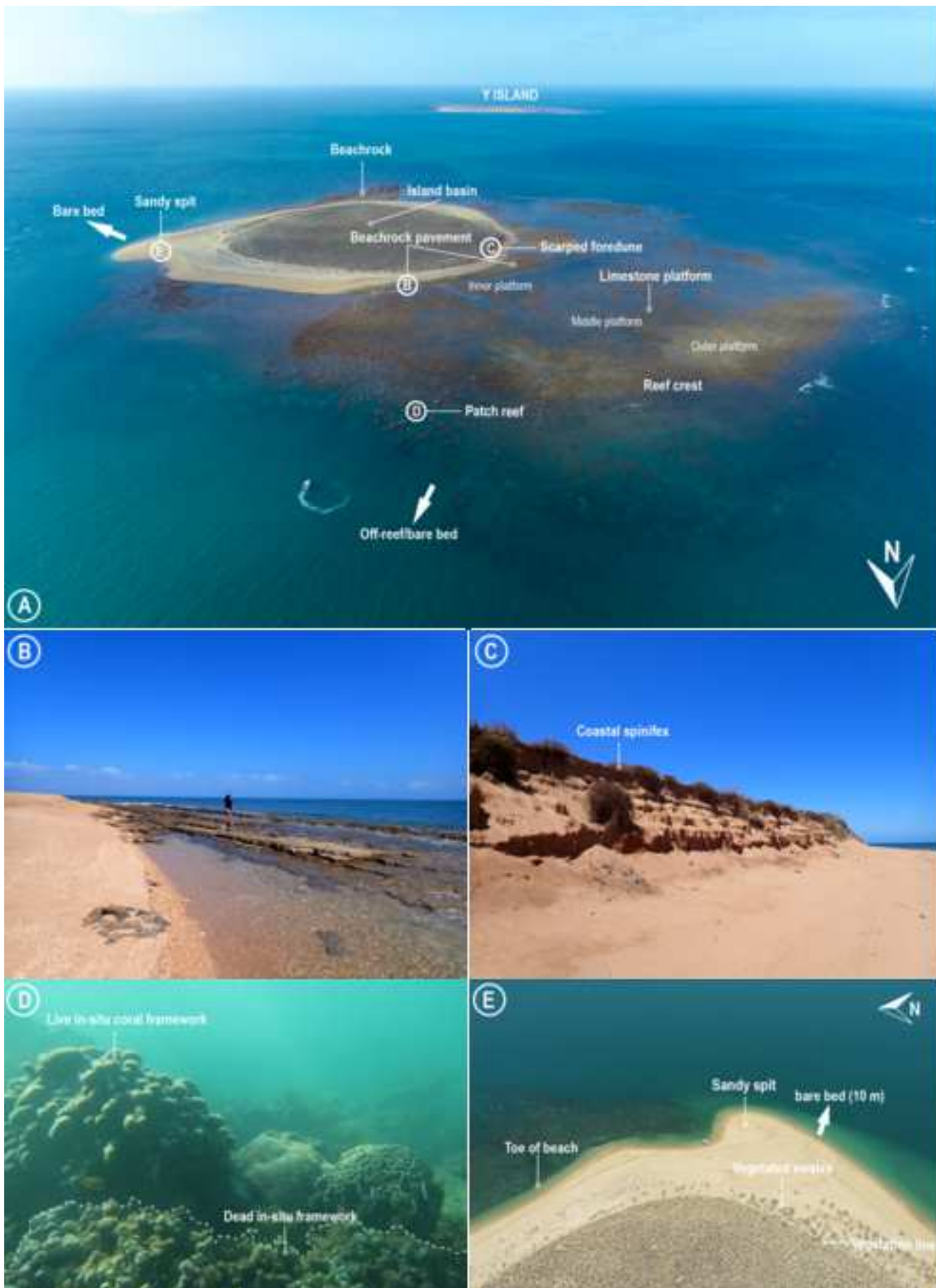
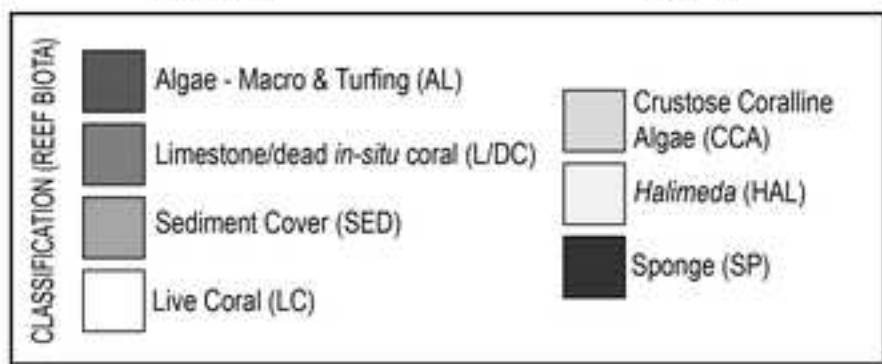
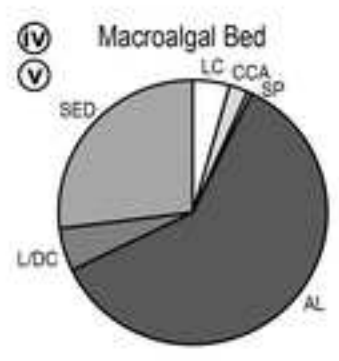
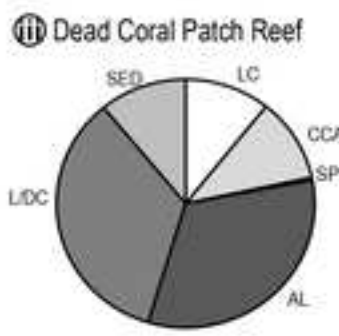
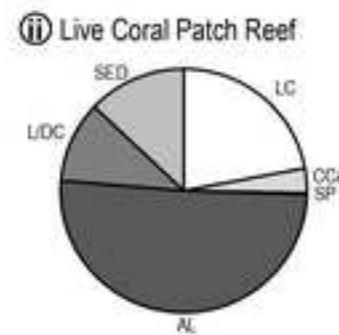
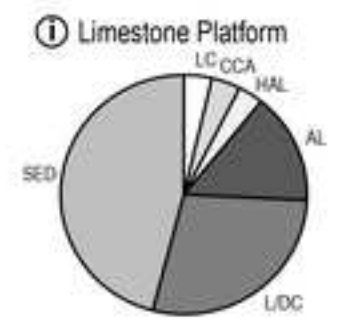
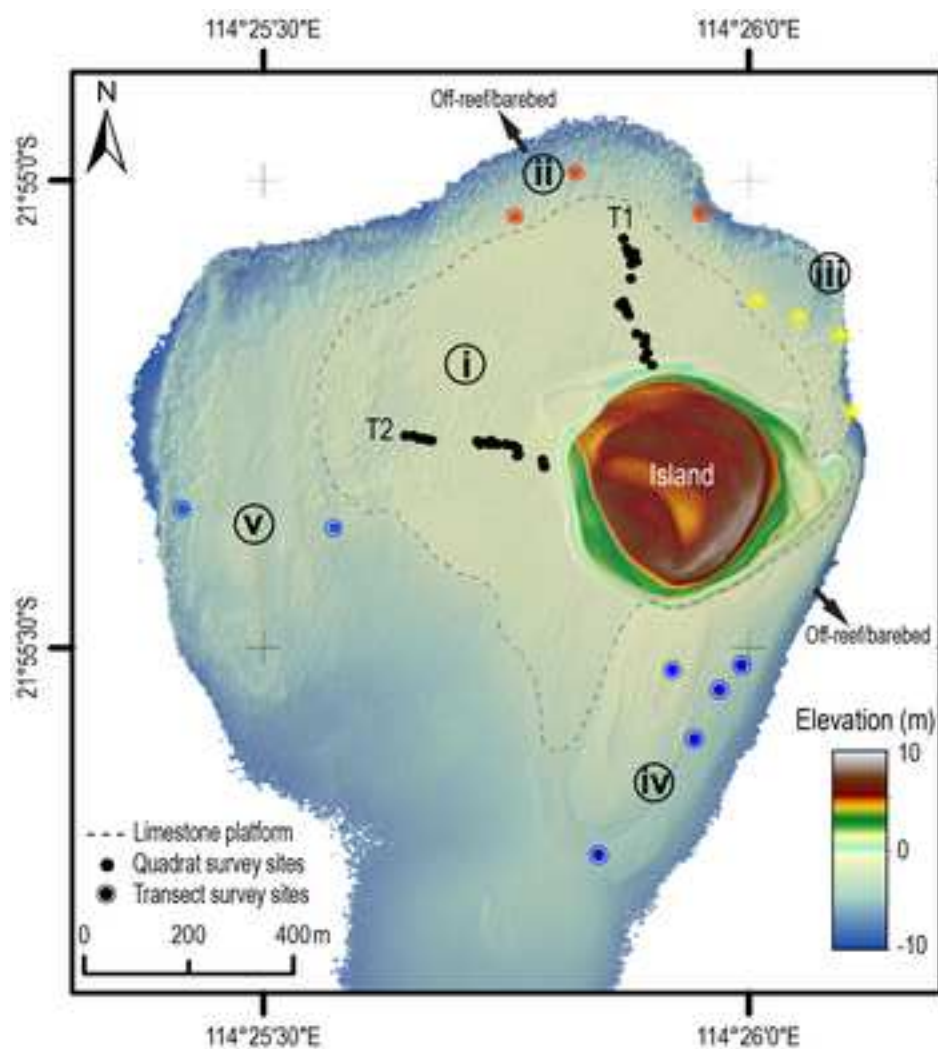


Figure 3.



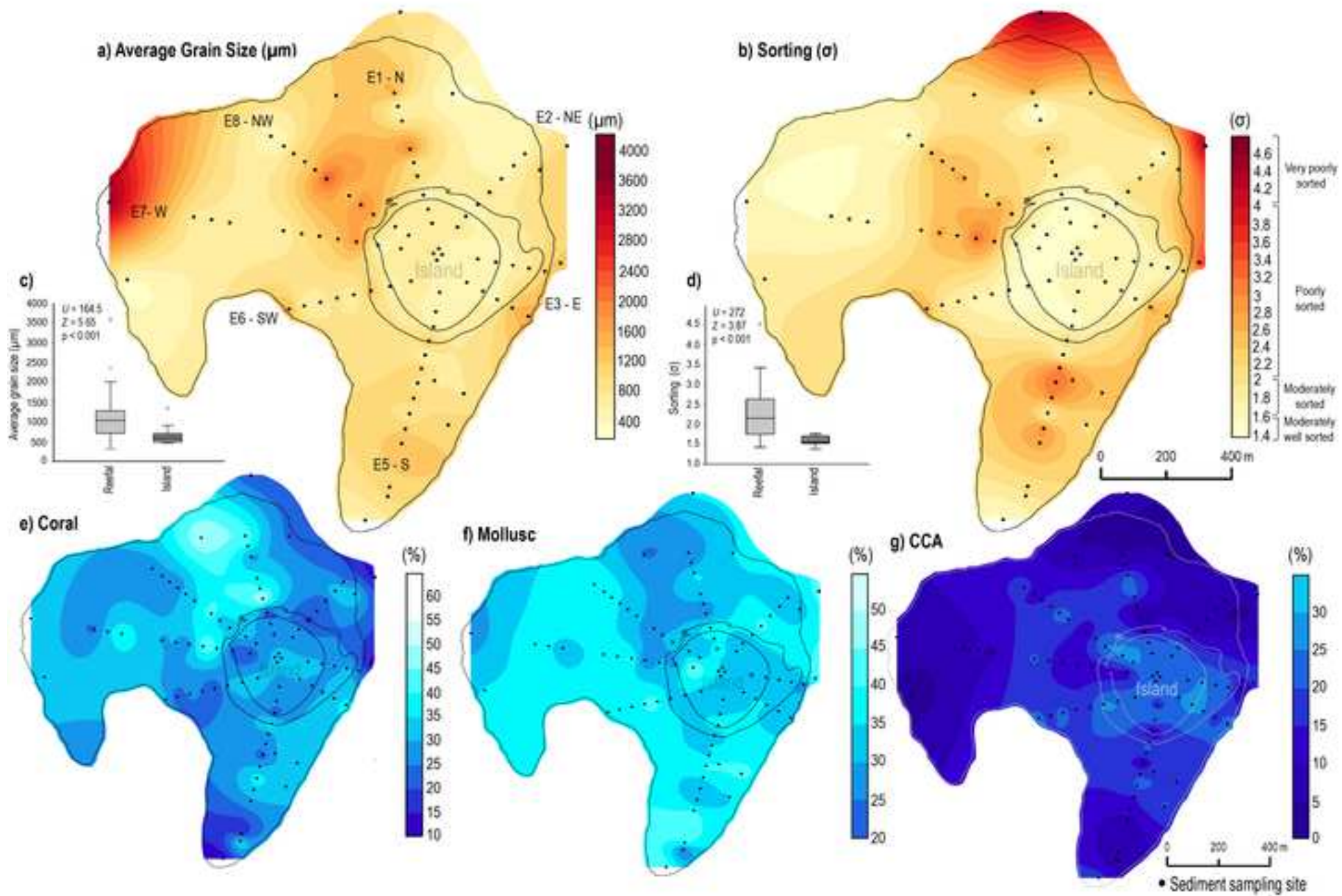
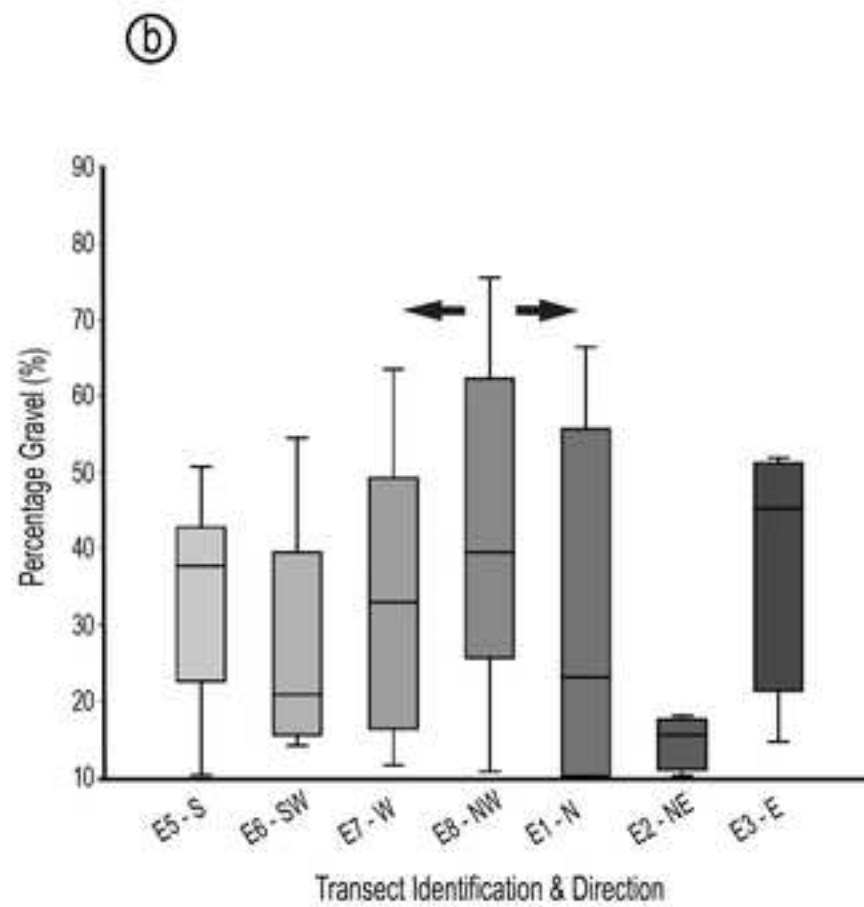
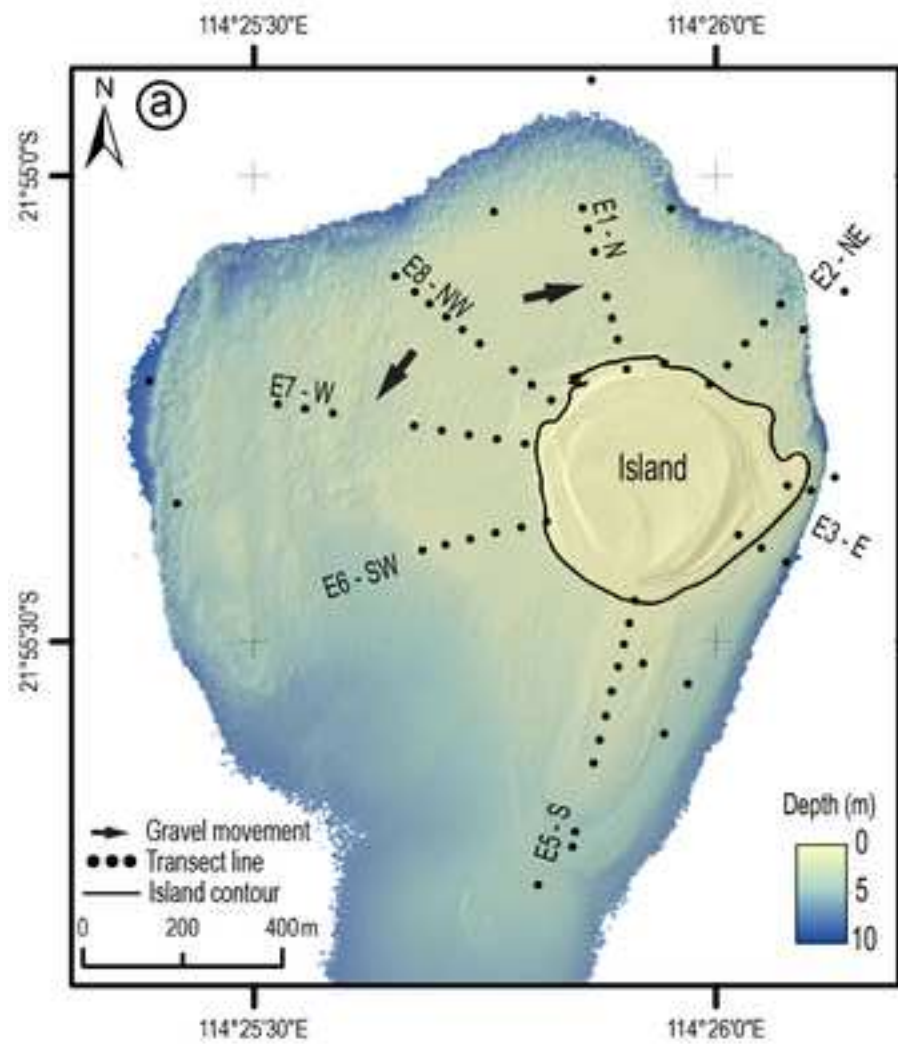
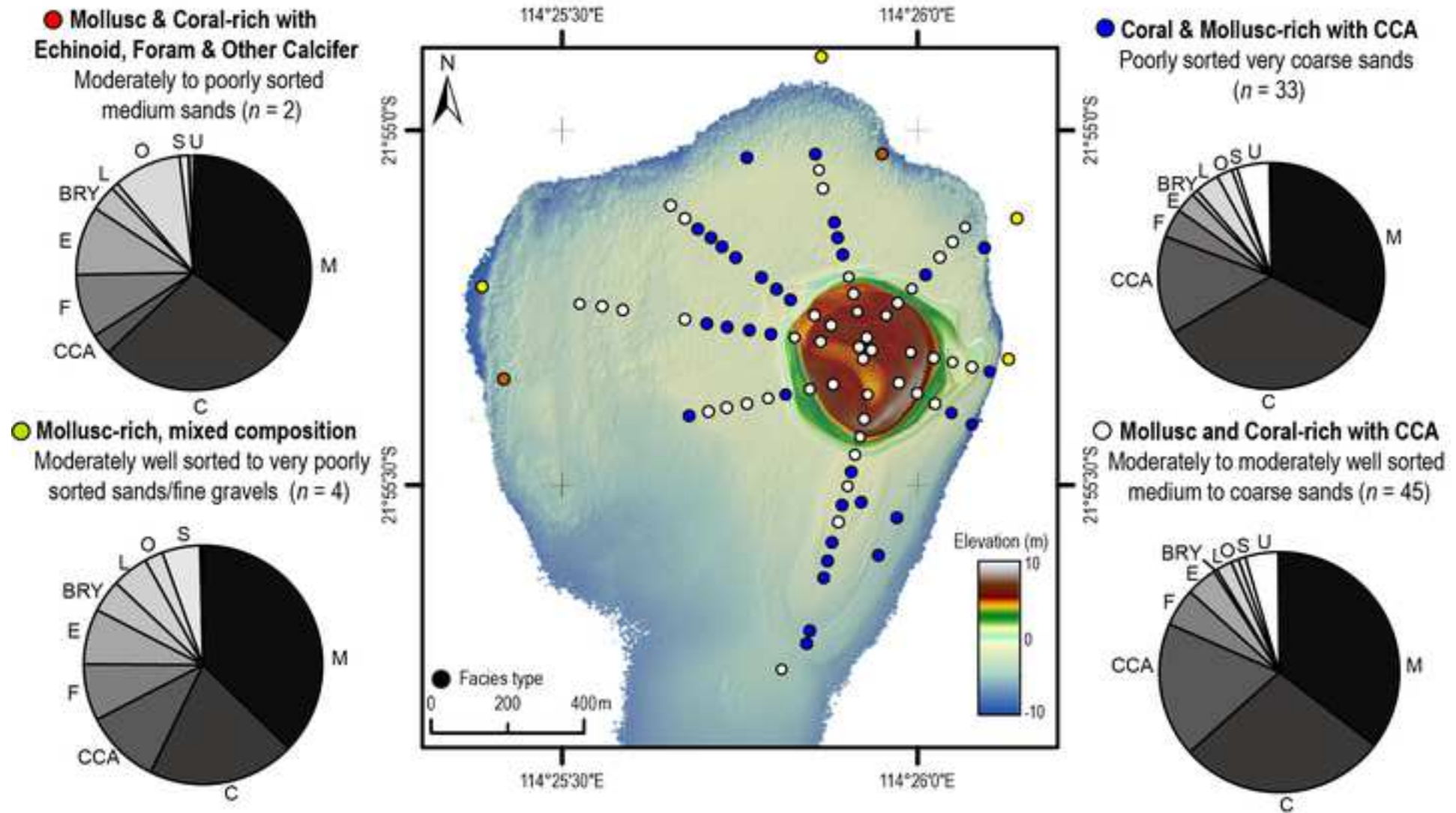


Figure 5.





Zone	(1) Limestone platform	(2) Live coral patch reef	(3) Dead coral patch reef	(4 & 5) Macroalgal beds	
Aspect	NE to West	North	East	South	West
Mean elevation range (m m.s.l)	-0.5 to - 1.2 m	-2 to - 2.5 m	-1.6 to -4 m	-2 to - 4.2 m	-2 to - 2.4 m
Dominant non-calcifying biota	<i>Sargassum, Padina & Dictyota sp.</i>	<i>Sargassum, Padina & Dictyota sp.</i>	<i>Sargassum, Padina & Dictyota sp.</i>	<i>Sargassum, Padina & Dictyota sp.</i>	<i>Sargassum, Padina & Dictyota sp.</i>
Calcifying biota	Small coral recruits of <i>Favites, Goniastrea, Pocillopora, Porites sp.</i> & CCA, <i>Halimeda</i> & mobile gastropods.	<i>Pavona, Turbinaria, Pocillopora, Acropora, Goniastrea, Favites & Porites sp.</i> , mobile gastropods	<i>Acropora, Montipora, Turbinaria, Astrea, Cyphastrea, Favites, Platygyra, Pocillopora, Porites sp.</i> & CCA, mobile gastropods.	Very sparse (single) colonies of <i>Turbinaria, Acropora, Montipora, Platygyra, Porites, Favites, Astrea and Coelastrea sp.</i>	<i>Sparse colonies of Acropora, Turbinaria, Pocillopora, Porites sp. & mobile gastropods</i>
Corals (no. colonies) including juvenile recruits*	n = 92	n = 144	n = 181	n = 77	n = 39
Molluscs (no. individual) including gastropods & sessile bivalves*	n = 26	n = 12	n = 11	n/a	n = 45
Echinoids (no. individuals)	n = 1	n = 2	n/a	n/a	n/a
Benthic Cover (%)					
Coral (%)	3.7 ± 0.4	23.0 ± 4.9	11.0 ± 4.9	4.1 ± 4.7	5.1 ± 0.6
CCA (%)	3.8 ± 1.2	3.3 ± 3.1	11.0 ± 5.5	1.8 ± 2.0	3.2 ± 4.5
<i>Halimeda</i> (%)	3.3 ± 0.9	-	-	-	-
Macroalgae (%)	14.9 ± 5.3	50.8 ± 44.3	32.6 ± 22.6	64.0 ± 3.3	51.9 ± 0.2
Sponge (%)	-	0.21 ± 0.18	0.36 ± 0.33	0.5 ± 2.0	0.6 ± 0.05
Reef Framework (%)	28.3 ± 10.1	10.7 ± 9.6	34.3 ± 20.8	4.8 ± 3.4	6.3 ± 8.9
Sediment Cover (%)	45.9 ± 5.6	12.9 ± 5.6	10.9 ± 7.5	25.0 ± 4.5	32.8 ± 13.1